Journal of Food Engineering 165 (2015) 82–92

Contents lists available at ScienceDirect

Journal of Food Engineering

journal homepage: www.elsevier.com/locate/jfoodeng

Structure characterization by means of rheological and NMR experiments as a first necessary approach to study the L-(+)-ascorbic acid diffusion from pectin and pectin/alginate films to agar hydrogels that mimic food materials

Maria D. De'Nobili [a], Ana M. Rojas [a], Michela Abrami [b], Romano Lapasin [c], Mario Grassi [c,*]

[a] Departamento de Industrias, Facultad de Ciencias Exactas y Naturales, University of Buenos Aires, Ciudad Universitaria, 1428 Buenos Aires, Argentina
[b] Department of Life Sciences, Cattinara University Hospital, Trieste University, Strada di Fiume 447, I-34149 Trieste, Italy
[c] Department of Engineering and Architecture, University of Trieste, Via A. Valerio 6, 34127 Trieste, Italy

ARTICLE INFO

Article history:
Received 1 December 2014
Received in revised form 13 April 2015
Accepted 9 May 2015
Available online 12 May 2015

Keywords:
Agar hydrogels
Pectin edible films
Pectin–alginate edible films
Ascorbic acid
Dynamic rheology
Low field NMR

ABSTRACT

Pectin (P) and pectin–alginate (PAL) edible films, developed for antioxidant preservation, were placed on agar cylinders, mimicking food materials, in order to understand the release of L-(+)-ascorbic acid (AA) from the films. To improve the release properties of polymeric systems, it is crucial to describe and understand the macro- and microscopic properties of the matrices. Rheological studies performed within linear and non linear frames permitted to select, among different polymer concentrations (0.50–2.00% w/w), a 2.00% w/w agar gel as food model as this system shows the higher pure elastic contribution. Rheological and Low Field NMR (LFNMR) tests performed on 0.50–2.00% w/w agar gels as well as on P- and PAL-films after exposure (up to 6 h) to 2.00%-agar gels, showed that in spite of the higher glycerol (plasticizer) content, P-network is characterized by more numerous calcium-junction zones than PAL-matrix. The determined average network mesh size ($\bar{\xi}$) for both of P- and PAL-films did not significantly change during 6 h of contact with 2.00%-agar gel. However, due to a higher swelling degree, PAL-film leads to higher $\bar{\xi}$ value and water mobility inside the polymeric network. These results are of paramount importance as "$\bar{\xi}$" is the main parameter affecting the release kinetics of AA from film networks to agar gels and also the diffusion of AA into the agar gel or food.

1. Introduction

Agar is a gel forming polysaccharide with a main chain consisting of alternating 1,3-linked β-D-galactopyranose and 1,4-linked 3,6 anhydro-α-L-galactopyranose units (Arnott et al., 1974). Agar can be fractionated into two components: agarose and agaropectin (Labropoulos et al., 2002). Agarose is a neutral polysaccharide and represents the fraction with the greatest gelling capacity. The other agar fraction, agaropectin, contains the charged polysaccharide components. Agarose and agaropectin contents depend on the seaweed source from which agar is extracted and it affects the physicochemical, mechanical and rheological properties of agar gels (Labropoulos et al., 2002). It has been suggested that the agarose network arises from double helix formation and subsequent aggregation of these helices into bundles, called suprahelices (Djabourov et al., 1989; Labropoulos et al., 2002). However, according to the molecular modeling study performed by Kouwijzer and Pérez (1998), agarose appears to be capable of forming both single- and double-helical structures, which are left-handed and antiparallel packed. Additionally, all of the proposed crystal structures show enough space (30–45%) that can be occupied by water molecules, fact that is expected for a gel-forming polysaccharide.

Edible films constitute an application of the active food packaging (Han, 2005). When stored at sufficiently low relative humidity values such as 57%, edible films made up by high methoxyl pectin and carrying L-(+)-ascorbic acid (AA) were excellent barriers to oxygen per se and produced additional antioxidant protection, preserving a functional food such as walnut oil from tocopherol and lipid oxidations (Pérez et al., 2013). Thus, food, as well as pharmaceuticals preservation can take advantage from edible films and coatings as they can be used to support active compounds (antimicrobials, natural antioxidants), while constituting controlled delivery systems with localized activity at interfaces. In previous works, films based on low methoxyl pectin (De'Nobili et al., 2011) and alginates (De'Nobili et al., 2013) were successfully developed to

* Corresponding author.
E-mail address: mario.grassi@di3.units.it (M. Grassi).

http://dx.doi.org/10.1016/j.jfoodeng.2015.05.014
0260-8774/

support and stabilize AA in view of antioxidant protection. Pectins are complex polysaccharides present in the primary cell walls of plants. They are rich in galacturonic acid and often contain significant amounts of rhamnose, arabinose and galactose as well as 13 other different monosaccharides (Vincken et al., 2003). Three major pectic polysaccharides domains are recognized: homogalacturonan (HG), rhamnogalacturonan I (RG-I) and rhamnogalacturonan II (RG-II) (Pérez et al., 2000; Willats et al., 2006). However, commercial pectins are mainly constituted by HG because lateral substitution of the RG-I kinks has been partially hydrolyzed during the extractive process (Voragen et al., 2009). As other biopolymers, pectins are able to form continuous crystalline and/or amorphous microstructures like films. On the other hand, alginate is a biomaterial that has found numerous applications in biomedical science and engineering (Lee and Mooney, 2012). Alginic acid is an unbranched binary copolymer extracted from brown algae, constituted by (1,4)-linked β-D-mannuronic acid units (MM-block), α-L-guluronic acid monomers (GG-block) and sequences of alternating β-D-mannuronic and α-L-guluronic acid (MG-block) (Jothisaraswathi et al., 2006). Physical and mechanical properties of alginate materials, as well as biocompatibility for tissue engineering developments (Klöck et al., 1997; Stabler et al., 2001) and capacity for AA stabilization (De'Nobili et al., 2013) are highly dependent on the relative content of G to M. Calcium ions can partly replace hydrogen bonding, zipping GG- (but not MM- or MG-) chains together stoichiometrically in an "egg-box" conformation (Braccini and Pérez, 2001).

Edible films can be placed on agar cylinders, mimicking food materials, in order to understand the release of AA from the edible films and the diffusion into the agar gel. It is well known that, in order to improve the release properties of polymeric systems, it is crucial to describe and understand the macro- and microscopic properties of the matrices (Grassi et al., 2007). For this purpose, a rheological study was carried out on samples of agar in order to analyse the effect that polymer concentration can exert on the macromolecular network and on the edible film/agar system at different times. Thus, stress sweep experiments were carried out to determine the linear viscoelastic range. Frequency sweep experiments were also performed and, applying the Flory's theory, an evaluation of the cross-linking density is given. From this value, according to the equivalent network model (Schurz, 1991), an estimation of the average mesh size, $\bar{\xi}$, of the hydrogel networks is given together with the dependence of this parameter on the agar concentration and the kind of polymer that form the edible film. Such microscopic parameter allows depicting a possible microscopic structure of the network, this being very important for the description of gel networks and very useful for understanding the delivery properties of this kind of matrices. In this frame, the aim of the present work was to characterize, by means of rheology and Low Field NMR (LF NMR), (i) the agar hydrogel at different polymer concentrations, (ii) the agar hydrogel (model of foods materials) after contact, for different times, with two pectin (P) and pectin–alginate (PAL) edible films and (iii) the P and PAL films after contact with agar hydrogel. Indeed, these two approaches can provide useful information about the polymeric chain architectures (polymeric networks) and their possible modifications during the release of AA while the edible film is in contact with the agar hydrogel.

2. Materials and methods

2.1. Agar cylinders

The agar cylinders were made at different concentrations (2.00%, 1.50%, 1.00%, 0.50%, 0.25% w/w) by respectively dissolving 2.00, 1.50, 1.00, 0.50 and 0.25 g of agar into enough distilled water (≈90 mL) at a temperature of 90 °C, after which the total weight was completed to 100.00 g in a scale (0.01 g precision). The solution was homogenized and poured into horizontally plates of 2–3 mm-height and then it was allowed to cool for gelling (37 °C). After its formation, the gel was cut into 35 mm diameter disks with a stainless-steel punch and used for rheology tests. For NMR tests, cylinders were cut using the LF-NMR tube as a punch and then piled up in order to obtain 20 mm-height × 8 mm-diameter agar cylinders.

2.2. Edible film formation

Films were made using casting technology. In order to constitute the P-films, an aliquot of 8.00 g of the low methoxyl pectin (GENU™ pectin type LM-12 CG, CP Kelco, USA) powder was slowly poured in 250 g of deionized water under high stirring conditions (1400 rpm) using a vertical stirrer model LH, Velp Scientifica, Italy), to avoid lumps and obtain homogeneous hydration of the powder. On the other hand, an aliquot of 4.00 g of alginate (Cargill, Mechelen, Belgium) and 2.70 g of the low methoxyl pectin powder were poured in the same conditions as for P system in order to develop PAL-films.

While the high speed stirring was performed, the obtained viscous, homogenous and transparent system was then heated to 90 °C on a hot plate. Glycerol was added (5.00 g for P system and 2.50 g for PAL system) as a plasticizer, followed by potassium sorbate (0.0300% w/w) (Sigma–Aldrich, USA) as an antimicrobial agent and AA (0.1000% w/w) (Merck, Argentina), both pre-dissolved in deionized water. When the temperature was again 90 °C, $CaCl_2{\cdot}2H_2O$ pre-dissolved in deionized water was added while stirring. The total weight of the system was then made to 300.00 g by adding enough deionized water, followed by stirring for homogenization. The foam formed in the hot solution was removed with a spatula. The hot solution underwent vacuum for 15 s to eliminate bubbles and then poured onto leveled polystyrene plates (7.00 g of solution per each 55 mm-diameter polystyrene plate). Plates were cooled for 20 min at room temperature and then air-dried in a convection oven for 2.5 h at 60 °C. The films obtained were cooled at room temperature, peeled from the polystyrene plates and stored under vacuum into Cryovac™ bags.

2.3. Edible films in contact with agar cylinders

In an experiment, six films of either P or PAL were placed on each one of six cylinders of agar of only one concentration selected among those above assayed (0.25–2.00% w/w). These systems (agar cylinder + film) were put into a container maintained at constant temperature (25.0 °C). At various time intervals (0.5, 1, 2, 3, 4, 5 and 6 h) one system was withdrawn each time and the film and the corresponding cylinder were separately weighed in order to monitor the kinetics of loss/gain of water. Both, the agar cylinder and the film were characterized by means of rheological and LF-NMR assays at each time. The experiment was made in triplicate.

2.4. Rheological investigations

The rheological characterization of films and agar hydrogels was carried out at 25.0 °C using a controlled-stress rheometer RS-150 (ThermoHaake, Germany) equipped with parallel plates (PP35 TI, diameter 35 mm) having serrated surfaces and provided with a Haake-F6 thermostat for temperature control. The measuring device was kept inside a glass bell at saturated humidity conditions to avoid evaporation effects. The agar (2.00%, 1.00%, 0.50%, 0.25% w/w) hydrogels (thickness of 2–3 mm) were removed

with the aid of a small spatula from the Petri dish in which they were prepared and were put on the lower plate of the measuring device. For the rheological characterization, each film was put on the lower plate covered with a high-grit sandpaper in order to offer a smoother surface to the thin film. The upper plate was then lowered until it reached the hydrogel surface. Gap setting optimizations have been performed according to the procedure described elsewhere (Kuijpers et al., 1999).

The viscoelastic properties of the samples were analyzed under oscillatory shear conditions by applying different procedures. Stress sweep tests (SS) were carried out at constant frequency (1 Hz) in order to determine the extension of the linear viscoelastic region and the pattern of the nonlinear viscoelastic response. Frequency sweeps tests (FS) were performed within the linear viscoelastic regime at constant deformation in the range of 0.01–50 Hz. The mechanical spectra obtained from FS tests were fitted to the generalized Maxwell model consisting of a parallel combination of Maxwell elements and a pure elastic element (G_e). Accordingly, the dependence of the elastic (G') and viscous (G'') moduli on pulsation ω is given by the following expressions:

$$G' = G_e + \sum_{i=1}^{n} G_i \frac{(\lambda_i \omega)^2}{1 + (\lambda_i \omega)^2} \tag{1}$$

$$G'' = \sum_{i=1}^{n} G_i \frac{(\lambda_i \omega)}{1 + (\lambda_i \omega)^2} \tag{2}$$

where $G_i = \eta_i/\lambda_i$, ω is the pulsation or angular frequency ($\omega = 2\pi f$), n is the number of Maxwell elements considered, G_i, η_i and λ_i represent, respectively, the elastic modulus, the viscosity and the relaxation time of the ith Maxwell element. The equilibrium modulus G_e measures the contribution of the purely elastic element. The simultaneous fitting of Eqs. (1) and (2) to experimental G' and G'' data was performed assuming that relaxation times (λ_i) were scaled by a factor 10 (Lapasin and Pricl, 1995). Hence, the parameters of the model were $2 + n$ (i.e. λ_1, G_e plus G_i ($1 < i < n$)). Based on a statistical procedure (Draper and Smith, 1966), n was selected in order to minimize the product $\chi^2 * (2 + n)$, where χ^2 is the sum of the squared errors.

Among other interesting information about macroscopic behavior (i.e. mechanical and relaxation spectra), rheological characterization allows also an estimation of the polymeric network nano-structure via the determination of the mean crosslink density ρ_x, defined as the moles of junctions between different polymeric chains per hydrogel unit volume in the swollen state. Indeed, Flory's theory (Flory, 1953) ensures that the following relation holds:

$$\rho_x = \frac{G}{RT}\left(\frac{v_p}{v_{p0}}\right)^{2/3} \tag{3}$$

where R is the universal gas constant, T is the absolute temperature, v_p and v_{p0} are, respectively, the polymer volume fraction in the swollen state and in the crosslinking state. The shear modulus G can be computed as the sum of the elastic contributions ($G = G_e + \sum_{i=1}^{n} G_i$, see Eqs. (1) and (2)) pertaining to each element of the generalized Maxwell model describing the hydrogel mechanical spectrum (Pasut et al., 2008). ρ_x knowledge, jointly with the equivalent network theory (Schurz, 1991), allows the estimation of the polymeric network $\bar{\xi}$. Indeed, the equivalent network theory, starting from the evidence that, in the majority of the situations, a detailed description of a real polymeric network is very hard if not impossible, suggests to replace it by an idealized network made up by a collection of spheres whose diameter coincides with the average network mesh size $\bar{\xi}$:

$$\bar{\xi} = \sqrt[3]{6/\pi \rho_x N_A} \tag{4}$$

where N_A is the Avogadro's number.

The following samples were analyzed:

(a) the matrix developed from different agar concentrations (0.25%, 0.50%, 1.00% and 2.00% w/w),
(b) the agar matrix of a selected concentration after being in contact for a given period (1 h, 2 h, 3 h, 4 h and 5 h) with either the P or PAL film,
(c) the P and PAL film matrices obtained in item (b).

2.5. Proton nuclear magnetic resonance (LF-NMR)

Hydrogel and film characterizations were performed at 25 °C through low field ^{1}H NMR methodology, by means of a Bruker Minispec mq20 (0.47 T, Germany). Two kinds of experimental tests were performed: (a) determination of the water protons transverse relaxation time inside the hydrogels (T_2) (b) determination of the water diffusion coefficient inside the hydrogel polymeric structure (D_g; also called water self-diffusion coefficient; Holz et al., 2000); water is the only mobile species as polymeric chains cannot diffuse).

T_2 measurements were performed according to the CPMG (Carr–Purcell–Meiboom–Gill) sequence with a 90–180° pulse separation of 0.25 ms (number of scans: 4; delay: 5 s). The T_2 discrete distribution was determined by fitting the time (t) decay of the experimental signal (I_s), related to the extinction of the x–y component of the magnetization vector (M_{xy}). Data fitting was carried out by Microsoft Excel Visual Basic, taking advantage of the Microsoft Excel built in "Solver function" by fitting the experimental value I_s with the theoretical estimation $I(t)$:

$$I(t) = \sum_{i=1}^{m} A_i e^{-\frac{t}{T_{2i}}} \qquad \left\langle \frac{1}{T_2} \right\rangle = \frac{\sum_{i=1}^{m} A_i/T_{2i}}{\sum_{i=1}^{m} A_i} \tag{5}$$

where t is time, A_i are the pre-exponential factors (dimensionless) proportional to the number of protons relaxing with the relaxation time T_{2i} and $\left\langle \frac{1}{T_2} \right\rangle$ is the average value of the inverse relaxation time of protons. Again, m was determined by minimizing the product $\chi^2 * (2m)$, where χ^2 is the sum of the squared errors and $2m$ represents the number of fitting parameters of Eq. (5) (Draper and Smith, 1966). The T_2 continuous distribution was determined according to the following equation:

$$I(t) = \int_{T_{2\min}}^{T_{2\max}} \left(a(T_2) \exp\left(-\frac{t}{T_2}\right)\right) \mathrm{d}T_2 \tag{6}$$

where $T_{2\max}$ (= T_{2H_2O} = 3007 ms; free water relaxation time at 25 °C (Coviello et al., 2013) and $T_{2\min}$ (= 0.1 ms; lowest detectable experimental value of T_2) indicate, respectively, the lower and upper values of the continuous T_2 distribution, $a(T_2)$ is the unknown amplitude of the spectral component at relaxation time T_2 and $e^{(-t/T_2)}$ represents the decay term. $a(T_2)$ determination required Eq. (6) fitting to the experimental I_s data. Thus, Eq. (6) was discretized according to the criterion suggested by Whittal and MacKay (1989):

$$I(t) = \int_{T_2^{\min}}^{T_2^{\max}} a(T_2) e^{(-t/T_2)} \mathrm{d}T_2 \approx \sum_{i=1}^{N} a_i(T_2^i) e^{(-t/T_{2i})} \left(T_2^{i+1} - T_2^i\right)$$
$$= \sum_{i=1}^{N} A_i(T_2^i) e^{(-t/T_{2i})} \tag{7}$$

where the range of the T_2 distribution ($T_{2\min} - T_{2\max}$) was logarithmically subdivided into $N = 200$ parts (higher N values have revealed to be unnecessary). Because of the noise disturbing the

measure of I_s, fitting procedure must not minimize the χ^2 statistic, but a smoothed version (χ_s^2):

$$\chi_s^2 = \sum_{i=1}^{N}\left(\frac{I_s(t_i) - I(t_i)}{\sigma_i}\right)^2 + \mu\sum_{i=1}^{N-2}|A_{i+2} - 2A_{i+1} + A_i|^2 \quad (8)$$

where σ_i is the ith datum standard deviation, μ the is weight of the smoothing term (second summation in Eq. (8)) proposed by Provencher (1982). Although different criteria can be followed for μ determination, in this case, the strategy adopted by Wang and Ni (2003) was undertaken. The chosen μ value (= 300) is that occurring just after the heel (slope variation) of the function $Ln(\chi_s)$ vs $Ln(\mu)$. Data fitting was led writing in Microsoft Excell Visual Basic a proper "User Defined Function" representing Eq. (7) and, then, taking advantage of the Microsoft Excel built in "Solver function".

The information coming from relaxation experiments were also used for the estimation of the mesh size distribution of our hydrogels. Indeed, on the basis of the Scherer theory (Scherer, 1994), Grassi et al. (2015) recently demonstrated that, for diluted gel systems (polymer volume fraction $v_p \leqslant 0.1$), the $\bar{\xi}$ can be expressed as:

$$\bar{\xi} = \sqrt{3\pi\frac{(1-v_p)}{v_p}}R_f \quad (9)$$

where R_f is the radius of the polymeric chain. In addition, the "Fiber-Cell" theory (Chui et al., 1995) ensures that the following relation holds:

$$\left\langle\frac{1}{T_2}\right\rangle = \frac{1}{T_{2H_2O}} + \frac{2}{f}\frac{\langle\mathcal{M}\rangle}{\bar{\xi}} \qquad f = \sqrt{\frac{1-v_p}{v_p 3\pi}} \quad (10)$$

where $\left\langle\frac{1}{T_2}\right\rangle$ is the inverse of the average relaxation time of the protons of the water molecules trapped within the polymeric network of the gel, T_{2H_2O} is the relaxation time of the protons of the bulk water (i.e. protons of the free water, whose relaxation is not affected by the presence of the polymeric chains; 3007 ms at 25 °C (Coviello et al., 2013) and $\langle\mathcal{M}\rangle$ (length/time) is an empirical parameter, called relaxivity, accounting for the effect of polymer chains surface on proton relaxations. While Eq. (10) holds on average for all the polymeric network meshes, similar expressions can be written for polymeric network meshes of different dimensions (ξ_i):

$$\frac{1}{T_{2i}} = \frac{1}{T_{2H_2O}} + \frac{2}{f}\frac{\langle\mathcal{M}\rangle}{\xi_i} \quad (11)$$

where T_{2i} is the relaxation time of the water molecules protons trapped in polymeric meshes of size ξ_i. ($\langle\mathcal{M}\rangle$ is retained ξ_i independent). Eqs. (10) and (11) hold in fast-diffusion regime, i.e. when the mobility of the water molecules, expressed by their self-diffusion coefficient D_g, is high compared to the rate of magnetization loss, identifiable with $\langle\mathcal{M}\rangle R_c$ (i.e., $\langle\mathcal{M}\rangle R_c/D_g \ll 1$). R_c, indicating the distance from the polymer chain axis where the effect of polymeric chains on water protons relaxation becomes negligible, can be expressed by:

$$R_c = \frac{R_f}{\sqrt{v_p}} \quad (12)$$

As $\langle 1/T_2\rangle$ (see Eq. (5)), T_{2H_2O}, f (see Eq. (10)) and $\bar{\xi}$ (see Eq. (9)) are known, Eq. (10) allows the determination of $\langle\mathcal{M}\rangle$. Furthermore, by knowing $\langle\mathcal{M}\rangle$ and T_{2i} (Eqs. (5)), (11) makes possible the evaluation of ξ_i for each class of network meshes. In addition, once $\langle\mathcal{M}\rangle$ and the continuous T_2 distribution $a(T_2)$ (see Eq. (7)) are known, it is possible determining the continuous ξ distribution $a(\xi)$. Indeed, the following relations hold:

$$\xi = \frac{2\langle\mathcal{M}\rangle}{f}\Big/\left(\frac{1}{T_2} - \frac{1}{T_{2H_2O}}\right) \quad (13)$$

$$a(\xi) = \frac{dT_2}{d\xi}a(T_2) = \frac{\sqrt{\frac{1-v_p}{v_p 3\pi}}}{2\langle\mathcal{M}\rangle}\left(\frac{T_{2H_2O} - T_2}{T_{2H_2O}}\right)^2 a(T_2) \quad (14)$$

In addition, for a better comparison among different gels, it is convenient defining the probability $P(\xi)$ of finding a mesh of size ξ inside the polymeric network:

$$P(\xi) = \frac{a(\xi)d\xi}{\int_{\xi_{min}}^{\xi_{max}} a(\xi)d\xi} = \frac{A(\xi)}{\int_{\xi_{min}}^{\xi_{max}} a(\xi)d\xi} \quad (15)$$

In order to gain further information about polymeric network structure, Pulsed Gradient Spin Echo (PGSE) measurements were performed. The applied sequence consisted of the classical CPMG sequence with two equal gradient pulses (of length δ = 0.5 ms) occurring at x_1 = 1 ms and x_2 = 1 ms after the 90° and 180° pulses, respectively. The time separation, indicated by Δ ($\approx \tau - x_1 - \delta + x_2$), is related to the water molecule diffusion time t_d according to $t_d \approx \Delta - \delta/3$. After a proper calibration procedure, based on the knowledge of the free water self-diffusion coefficient (D_{H_2O}) (Coviello et al., 2013) it is possible to measure the average water self-diffusion coefficient inside the hydrogel (D_g). Interestingly, for sufficiently long t_d (this happens when D_g is no longer dependent on t_d; for smaller t_d, D_g decreases with increasing t_d) the ratio between D_{H_2O} and D_g identifies with the polymeric network tortuosity (α) (Latour et al., 1993).

The samples analyzed were the same as those indicated for the rheological investigation.

2.6. Statistical analyses

The results are reported as the arithmetical mean and standard deviation for n (number of replicates) (Sokal and Rohlf, 2000). When necessary, the statistical analyses of results were performed by applying ANOVA (α: 0.05), followed by pairwise multiple comparisons evaluated by Tukey's significance difference test. Data fitting was carried out through Microsoft Excel Visual Basic (Version 97-2003, USA), taking advantage of the Microsoft Excel built in "Solver function", and minimizing the error.

3. Results and discussion

3.1. Agar gel as a model system of viscoelastic solid food

Systems of increasing agar concentration were separately submitted to dynamic tests at 25.0 °C. Particularly, Fig. 1 shows the results obtained from strain sweep tests performed at 1 Hz. It can be noticed that the linear viscoelastic region, where both moduli do not depend on strain amplitude (γ), is more visible for the higher agar concentrations. The upper limiting strain (called critical strain, γ_{cr}) is progressively reduced to lower values as agar concentration increases from 0.25% to 2.00% w/w. Beyond γ_{cr}, in the non linear regime, G' decreases monotonically with increasing strain in all the cases examined (2.00%, 1.00%, 0.50%, 0.25% w/w), whereas G'' firstly increases and then decreases, thus showing an overshoot in its profile. As the agar concentration increases, the overshoot is more evident. Such a large amplitude oscillatory shear (LAOS) behavior was classified as type III (weak strain overshoot) by Hyun et al. (2002). Stress or sweep tests have normally been used purely to find out the extension of the linear region before performing a frequency sweep test, and then non-linear data have been often neglected. Nevertheless, such tests can reveal the diverse characteristics of the rheological behavior of polymer solutions and hydrogels through the different patterns of both moduli

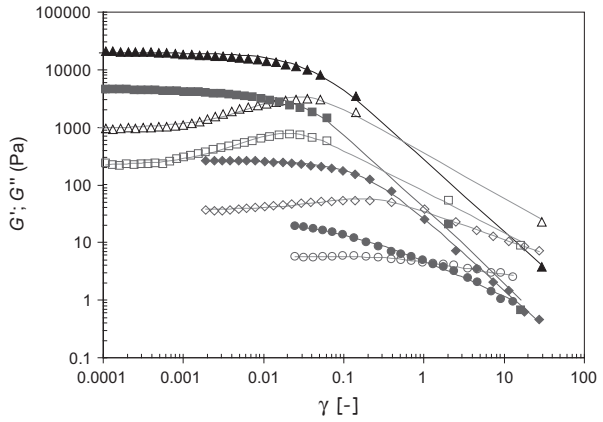

Fig. 1. Storage G' (filled symbols) and loss G'' (empty symbols) moduli recorded in the strain sweep tests (1 Hz; 25.0 °C) for different agar concentrations: 2.00% (▲), 1.00% (■), 0.50% (♦), 0.25% (●) w/w). Solid lines indicate the best fitting of Eq. (16). Experimental points correspond to three ($n = 3$) replicates.

in the nonlinear region. The microstructural differences resulting from molecular features and, even more, from inter-chains interactions and associations reflect into different rheological behaviors and these differences become more pronounced under large deformations.

At concentrations above 0.25%, the agar systems exhibit the typical behavior (type III) of several physical polymeric gels and other structured systems (colloidal dispersions of aggregated particles, block copolymer micellar systems, concentrated emulsions and filled polymers) (Lapasin et al., 2001). Upon cooling, the random coil-helix transition of agar chains and the subsequent association of single- or double helices give rise to higher ordered thermoreversible structures (Kouwijzer and Pérez, 1998). At sufficiently high concentration, they give rise to a three-dimensional gel network pervading the whole system from wall to wall. When an external strain is imposed, the inter-helical associations resist against deformation up to γ_{cr}, where G'' begins to increase owing to progressive structural rearrangements induced by increasing strain. Then, when G'' decreases, the complex structure undergoes a substantial breakup so that significant displacements and relative movements between polymer chains can take place and appreciable flow conditions are established.

In principle, such a strain-induced structural process postulated for agar gel systems could be mathematically described by the network model, which has been proposed by Sim et al. (2003) to provide a comprehensive interpretation and description of the main four types of LAOS behavior. According to this model, the differences between them come out from different sign and values of the parameters characterizing the creation and loss rates of network junctions. Type III behavior occurs when both the creation and loss rate parameters are positive but the creation rate parameter is smaller than the loss rate parameter. However, it must be underlined that the structural cause of the strain overshoot behavior in G'' is not universal, depending on the class of soft material under investigation, and, then, the network model cannot provide a funded physical interpretation of the structural mechanism on molecular scale. Alternatively, the strain dependence of both moduli can be satisfactorily described with the following equation (Lapasin et al., 2001):

$$G = G_0 \frac{1 + a\gamma}{1 + (b\gamma)^n} \tag{16}$$

where G_0 represents the limiting value of the modulus (G' or G'') in the linear conditions. For $a = 0$, it reduces to the Soskey–Winter equation (Soskey and Winter, 1984), which is suitable to describe only the monotonic decay of the G'. Table 1 reports the values of the parameters derived from data fitting. G'_0 and G''_0 increase with concentration according to simple scaling laws. The scaling exponent of G' is higher than that of G'' (3.2 vs 2.4), and this underlines the increasing elastic character of the agar gel with increasing concentration. The increase of the parameter a'' with increasing concentration underlines how the G'' overshoot becomes more pronounced at concentrations of 1.00% and above. In such conditions, the intermolecular interactions and associations are much more numerous and effective at higher concentrations, so preventing or contrasting the relative motion of the chains or structural units that constitute the system. The rate of decrease of both moduli in the nonlinear region is measured by the parameters n' and n'' (Table 1) whose values become more pronounced at higher concentrations.

The critical strain γ_{cr}, marking the border of the linear viscoelastic region, can be arbitrarily associated with the following criteria:

$$G' = 0.95 \cdot G'_0, \quad G'' = 1.05 \cdot G''_0$$

and then determined as the average of the two values calculated from the equation parameters. As it can be seen in Table 1, its value decreases with increasing concentration, whereas the corresponding critical stress (σ_{cr}) increases following a scaling law whose exponent is close to 2.

Frequency sweep tests were carried out at constant stress within the linear viscoelastic regime. Fig. 2 sums up the effect of polymer concentration on the linear viscoelastic behavior of the agar systems. In all the cases, the G' is almost independent of the angular frequency ω (scaling exponent between 0.035 and 0.060) and greater than G'' in more than one order of magnitude at higher agar concentrations. The mechanical spectra of the most concentrated systems are typical of strong gels having highly elastic character (Lapasin and Pricl, 1995). A satisfactory data correlation is provided by the generalized Maxwell model (with five Maxwell elements) as it can be seen in Fig. 2. The best fitting parameters of the model are reported in Table 2. Apart from higher G_i moduli, the $C_p = 2.00\%$ w/w of agar gel differs from the $C_p = 0.50\%$ and $C_p = 0.25\%$ samples mainly for a higher pure elastic contribution (see Table 2). Consequently, the agar concentration of 2.00% w/w was selected to develop hydrogel samples as the viscoelastic solid food model to be placed in contact with pectin and pectin–alginate edible films.

Table 1
Parameter values obtained from the strain dependence of both the elastic (G') and loss (G'') moduli fitted by the equation modified by Lapasin et al. (2001).[a]

	Agar concentration (% w/w)			
	2.00%	1.00%	0.50%	0.25%
G'_{0i} (Pa)	19,436	4168	260	26
a'	0	0	0	0
b'	26.9	29.2	5.60	9.54
n'	1.27	1.35	1.28	0.67
G''_{0i} (Pa)	963	218	37	6
a''	207	319	11.0	0.04
b''	34.6	51.6	5.28	0.23
n''	1.79	1.72	1.48	0.77
$\gamma_{cr,mean}$ (–)	0.0019	0.0020	0.011	0.023
$\sigma_{cr,mean}$ (Pa)	37.9	8.44	2.96	0.630

[a] For $a = 0$, Lapasin's equation reduces to the Soskey and Winter's equation (Soskey and Winter, 1984), which only describes the monotonically decay of G'.

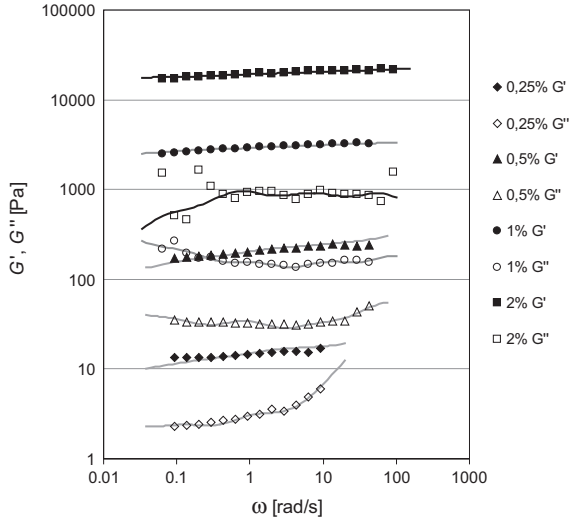

Fig. 2. Mechanical spectra of the agar systems at different concentrations. Squares and circles represent storage (G') and loss (G'') moduli, respectively. Solid lines indicate the best fitting of the generalized Maxwell model [Eqs. (1) and (2)] composed of six elements. Experimental points correspond to three ($n = 3$) replicates.

3.2. Study of the selected 2.00% agar hydrogel after being in contact for different periods with either pectin or pectin–alginate edible films supporting L-(+)-ascorbic acid

Strain sweep tests were performed at a constant frequency of 1 Hz (25.0 °C) on the chosen 2.00% w/w-agar gel cylinders on the face that was previously in contact for a given time (0–5 h) with either a P or a PAL film sample (Fig. 3). The linear viscoelastic region is clearly observed up to a shear strain of ≈0.01–0.015. After the linear region, G' decreases monotonically with the increase in the shear strain γ whereas G'' shows an overshoot in its profile, for all contact periods assayed (0, 1, 2, 3, 4 and 5 h) (Fig. 3). As previously determined, a type III-LAOS profile is hence observed for the 2.00% w/w agar hydrogels after each individual contact with either P or PAL film. The dependence of G' and G'' moduli on the shear strain can be described by Eq. (16) (Lapasin et al., 2001), as shown by the continuous lines drawn in Fig. 3. The parameters obtained by fitting are then summarized in Table 3. The G'_0 and G_0'' moduli of the 2.00% w/w agar gel samples are almost constant up to 5 h of contact with each kind of film studied. G'_0 and G_0'' values obtained from the agar gels tend to be slightly lower after 5 h of contact with the PAL film sample than with the P film (Table 3). Parameter a'', in general, decreases for increments in the contact time with both films. The rate of decrease of both moduli in the nonlinear region measured by the n' and n'' parameters in general does not change after different periods of contact with films, except at 1 h of agar gel touching with PAL film ($n'' = 4.02$) (Table 3).

Table 2
Frequency sweep parameters obtained according to the generalized Maxwell model assuming G_e, λ_1 and G_i as fitting parameters (first fitting strategy). C_p corresponds to the agar concentration.

	C_P (% w/w)			
	2.00	1.00	0.50	0.25
G_e	17,490	1947	31	6
λ_1	0.00199	0.00860	0.01159	0.00835
G_1	4014	317	102	75
G_2	726	204	34	0
G_3	1368	200	49	4
G_4	1409	259	43	3
G_5	664	618	101	5

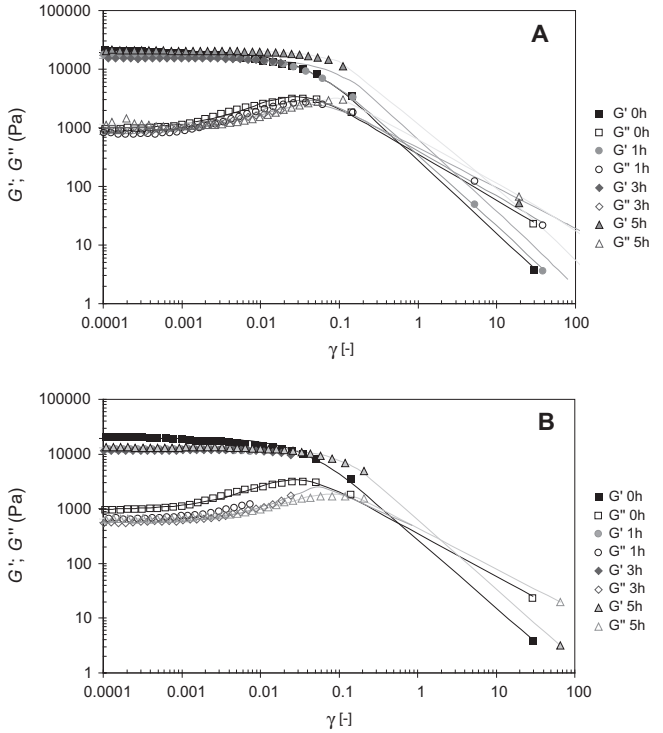

Fig. 3. Storage G' (square symbols) and loss G'' (circles) moduli recorded in the strain sweep tests (1 Hz; 25.0 °C) performed on the 2.00% w/w agar hydrogel cylinders after being in contact for different periods with either the pectin (A) or pectin–alginate (B) film. Solid lines indicate the best fitting of the Eq. (16). Experimental points correspond to three ($n = 3$) replicates.

Table 3
Parameter values obtained from the strain dependence of both the elastic (G') and loss (G'') moduli determined in 2.00% w/w agar hydrogels after being in contact with pectin or pectin–alginate films, fitted by the equation modified by Lapasin et al. (2001).[a]

	0	1	2	3	4	5
Contact time (h) with pectin films						
G'_{0i} (Pa)	19,436	17,151	14,971	15,129	18,228	20,692
a'	0	0	0	0	0	0
b'	26.9	22.7	7.46	9.5	10.00	6.65
n'	1.27	1.24	1.31	1.31	1.25	1.27
G''_{0i} (Pa)	963	769	880	882	876	1143
a''	207	180	167.0	104.1	56.9	52.6
b''	34.6	27.07	14.38	22.9	14.3	8.9
n''	1.79	1.77	1.75	1.69	2.13	1.83
Contact time (h) with pectin–alginate films						
G'_{0i} (Pa)	19,436	12,391	12,814	11,626	13,160	15,760
a'	0	0	0	0	0	0
b'	26.9	30.2	5.15	17.5	7.82	7.78
n'	1.27	1.38	1.52	1.98	0.93	1.33
G''_{0i} (Pa)	963	668	562	557	782	651
a''	207	112	36.2	94.1	44.7	52.6
b''	34.6	6.65	7.52	12.2	10.8	11.4
n''	1.79	4.02	1.76	1.92	1.25	1.76

[a] For $a = 0$, Lapasin's equation reduces to the Soskey and Winter's equation (Soskey and Winter, 1984), which only describes the monotonically decay of G'.

3.3. Study of the pectin and pectin–alginate films after contact with 2.00% agar hydrogel

Fig. 4 shows the strain sweeps carried out at a constant frequency of 1 Hz (25.0 °C) on the P and PAL film samples, which were previously in contact for a given period (0–5 h) with the 2.00% w/w-agar gel cylinders evaluated in Section 3.2. Depending on

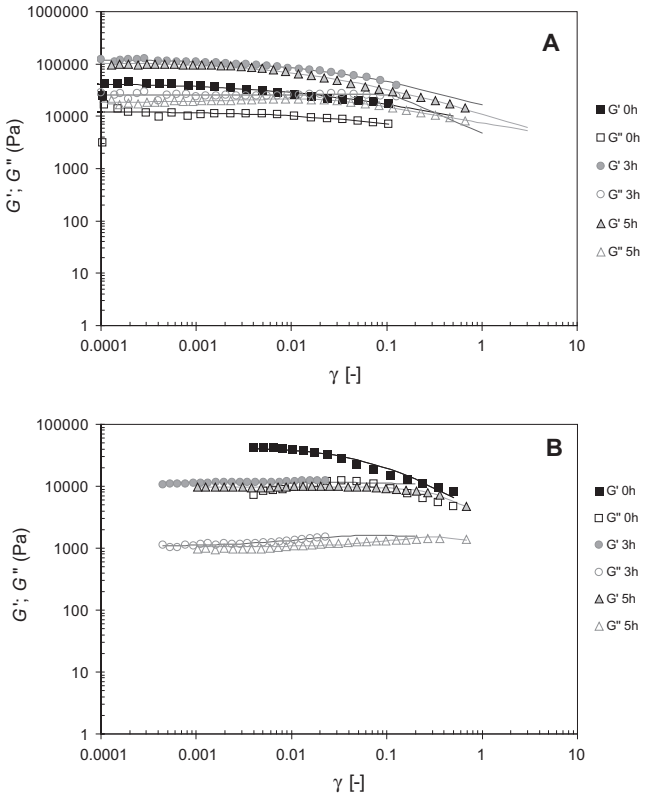

Fig. 4. Storage G' and loss G'' moduli recorded during the strain sweep tests (1 Hz; 25.0 °C) performed on either the pectin (A) or pectin–alginate (B) film, which were previously in contact for different periods with 2.00% w/w agar hydrogel cylinders. Experimental points correspond to three ($n = 3$) replicates.

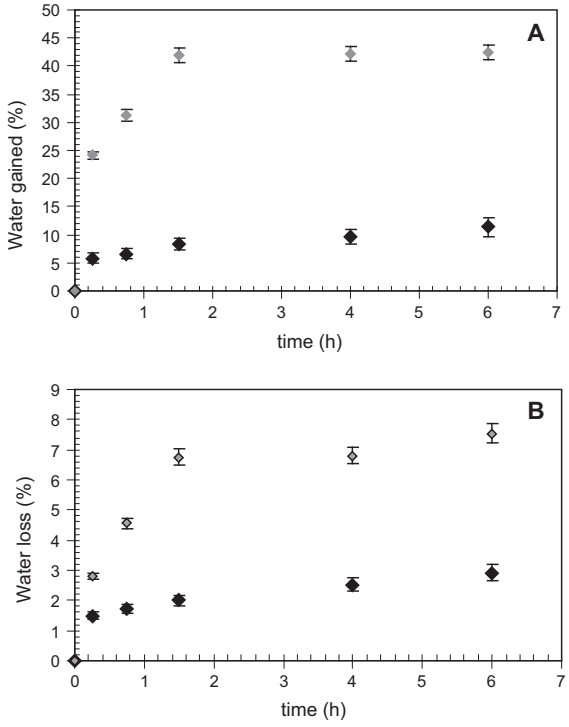

Fig. 5. (A) Water gained (swelling) by either pectin (♦) or pectin–alginate (◆) film after contact for the indicated time with 2.00% w/w-agar gels. (**B**) Water loss suffered by the 2.00% w/w-agar gels after having been in contact for the indicated time with either pectin (♦) or pectin–alginate (◆) film. Error bars correspond to the standard deviation ($n = 3$).

the contact period assayed, the linear viscoelastic region is observed up to a shear strain of ≈0.001–0.003 for P films and up to 0.008 and 0.04 for PAL films. G' was higher than G'' along the linear viscoelastic region for both kind of films and all contact periods assayed (Fig. 4). On the other hand, G' values obtained from films (Fig. 4) are one order of magnitude higher than those shown by the 2.00% w/w-agar hydrogel, for all contact periods of P films and at 0 h of contact of PAL film (Fig. 3). These results indicate the existence of a higher number of physical interactions between the film network macromolecules than between hydrated agar gel macromolecules. Calcium-junction zones of pectin and pectin–alginate film matrices are then stronger, especially after dehydration for film casting. At the different contact periods studied, G' values are in general higher for P film than for PAL films. Hence, the pectin network of P film is characterized by a higher number of calcium-junction zones than the pectin–alginate network of PAL film (Fig. 4), in spite of the higher glycerol (plasticizer) content of P film. As the contact period with 2.00% w/w agar gel increases from 0 to 3 h, the G' value determined on the P and PAL films in the linear viscoelastic region decreases (Fig. 4). As shown in Fig. 5A, the P and PAL films have gained the highest percentage of water (10% by P film and 40% by PAL film) at 3 h of assay. After the linear region, G' decreases monotonically with strain increasing and approaches G'' (Fig. 4), whereas G'' shows a slight overshoot in its profile, for all contact periods studied (0, 1, 2, 3, 4 and 5 h) (Fig. 4). Thus, a type III-LAOS profile is also observed for the P and PAL films after their respective contact with the agar gel, and experimental data fitted to Eq. (16) as demonstrated by the continuous line in Fig. 4. The limiting values of the G' or G'' modulus in the linear conditions, G_0, plotted against time of contact are shown in Fig. 6. It is observed that, for P film, G'_0 is almost independent of the time of contact with the agar gel, while it decreases for longer touching periods in the case of PAL film. During contact for longer periods, water significantly swells the PAL matrix (40%; see Fig. 5A), therefore affecting considerably the film microstructure. On the other hand, the proportion of water absorbed by the pectin network is noticeably lower (12%; see Fig. 5A), and higher G'_0 values than for PAL film are then observed (Fig. 6). This means that a higher number of physical interactions exist between the less hydrated pectin chains. Consequently, P film seems to be more useful as an interface applied on intermediate moisture foods since it maintains its nanostructure during contact due to the lower water absorption capacity. Probably, the higher content of glycerol (plasticizer) can contribute to avoid higher water absorption. In spite of its higher glycerol content per gram of pectin, the G' value determined through dynamic rheometry

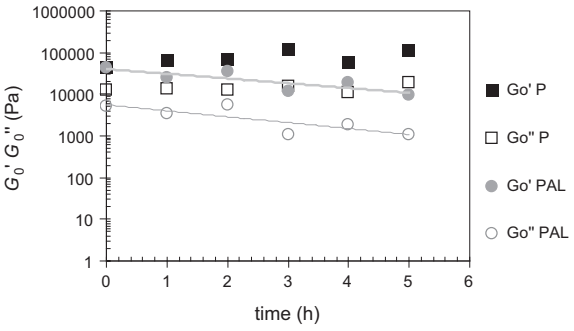

Fig. 6. The limiting values of the elastic (G'_0) and viscous (G''_0) moduli determined through Eq. (16) on pectin (P) and pectin–alginate (PAL) films after having been in contact with the 2.00% w/w-agar gels by the periods shown in the x-axis, are presented. Trend lines are plotted for the moduli determined on PAL film. Error bars for standard deviation ($n = 3$) are lower than the symbol size used.

was similar to that observed for PAL films before contact (0 h) with the 2.00% w/w agar gel (Fig. 4A and B).

3.4. Network characteristics of the agar hydrogel and edible films

Similarly to that occurring with chemically crosslinked polymers, recent results have shown that very stiff biopolymers might give rise to networks which are suitably described by a purely entropic approach, which holds when small deformations are considered, that is, under linear viscoelastic range (Turco et al., 2011). Hence, according to the rubber elasticity theory of Flory, the number (per unit volume) of elastically active chains or crosslink density (ρ_x) can be calculated from the shear elastic modulus, G, according to Eq. (3). In turn, Eq. (4) allows the estimation of the $\bar{\xi}$ of the polymeric network. Table 4 shows the inverse relationship between $\bar{\xi}$ (= $\xi_{i\,R}$) and the agar concentration used for gel development, which is in accordance with the G_0' increase with the agar concentration (Table 1). Average mesh size values ($\bar{\xi} = \xi_{i\,R}$) between 7.1 and 13.3 nm were determined for agar concentrations decreasing from 2.00% to 1.00% w/w. The LF NMR approach reveals that, whatever the agar concentration (see Table 4), only one relaxation time is needed to describe the water protons magnetic relaxation. This means that the polymeric network structure, hosting the water molecules, is homogeneous in term of mesh size distribution. Indeed, if it were not the case, more than one relaxation time would appear (Abrami et al., 2014). In addition, correctly, the higher the agar concentration, the smaller the relaxation time. This simply reflects the fact that the increase of polymer concentration in the gel implies a reduction of the average network mesh size (see Eq. (10)). The evaluation of D_g in hydrogel reveals that the polymeric network cannot heavily hinder the water molecules diffusion as the measured D_g values are not so far from the free water self diffusion coefficient at 25 °C (2.3×10^{-9} m^2/s; Holz et al., 2000). Consequently, from the water molecules point of view, this polymeric network is almost regular as its α is close to one (see Table 4). Additionally, as it was experimentally observed that D_g is constant with the diffusion time (t_d; data not shown), we can conclude that the mean size of the polymeric network mesh is very small (falling in the nano-range) and that network meshes are interconnected. If it were not the case, D_g would be a decreasing function of t_d (Latour et al., 1993). These qualitative considerations are supported by the evaluation of the average mesh size according to Eqs. (10) and (11). Table 4 shows that $\bar{\xi}$ (= $\xi_{i\,N}$) spans from about 24.8 nm to 17.4 nm. These values are not so far (about two times) from those determined by the rheological approach (Table 4, $\xi_{i\,R}$) also because they represent an average value. Looking at the continuous mesh size distribution (Fig. 7), in the case of the agar gel characterized by a 2% polymer concentration, we can see that the $\bar{\xi}$ rheological evaluation (= $\xi_{i\,R}$), practically, represents the smallest values of the size distribution evaluated by the LF NMR approach. Finally, it is important to underline that the use of Eqs.(10) and (11) is fully authorized due to the very small values assumed by the dimensionless parameter $\langle\mathcal{M}\rangle\, R_c/D_g$, this ensuring to be in the fast diffusion regime.

The effect of the agar gel facing, for different times, to initially dry P or PAL films can be seen, respectively, in the second and third part of Table 4. In the case of pectin films, we can see that limited water loss from the gel matrix (see Fig. 5B) does not qualitatively modify the agar network organization. The gel is characterized by only one relaxation time (T_{2i}) whose value is substantially constant over the 6 h of the test. In addition, the relaxation time value is smaller than that corresponding to the original agar gel (65 ms) and this could be attributed to the water loss experienced by the agar gel upon contact with the dry pectin film. Consequently, the average mesh size $\bar{\xi}$ ($\xi_{i\,N} \approx 15$ nm) is almost constant with time and it is smaller than that competing to the native agar gel (17.4 nm). Also in this case, the LF-NMR evaluation of $\bar{\xi}$ ($\xi_{i\,N} \approx 15$ nm) is about two times that coming from the rheological approach ($\xi_{i\,R} \approx 7$ nm). Finally, the measurement of D_g indicates that meshes are interconnected (D_g is t_d independent) and that water loss implies a reduction of the water mobility inside the polymeric network (this, in turn, means an increase of the network tortuosity with respect to the native agar gel). Also in this case, the values assumed by the dimensionless parameter $\langle\mathcal{M}\rangle\, R_c/D_g$ guarantees the fast diffusion regime, i.e., the safe use of Eqs. (10) and (11). On the pectin film side, the effect of the water gained from the agar gel is to considerably increase the water protons relaxation time that increases from about 2 ms (dry state) to about 14 ms of the swelling states (see Table 5). While the relaxation time in the dry state is due to the unavoidable humidity present in the pectin network (the LF-NMR sequence adopted for the relaxation experiments cannot detect the very fast relaxation time of polymer chains protons), the relaxation time of the swelling states is due to the liquid water absorbed by the agar gel. The fact that this relaxation time does not substantially change with the contact time is in agreement with the almost complete pectin film swelling

Table 4
Low field NMR parameters referring to the agar gels studied. T_{2i} and A_i are, respectively, the ith water protons relaxation time and its relative abundance, $\langle\mathcal{M}\rangle$ is relaxivity, $\langle\mathcal{M}\rangle\, R_c/D$ is a dimensionless parameter indicating fast diffusion conditions when it is $\ll 1$, $\xi_{i\,N}$ and $\xi_{i\,R}$ are, respectively, the average mesh size according to the low filed NMR and the rheological approach, D_g is the water self diffusion coefficient inside the gel and α is the polymeric network tortuosity.

	T_{2i} (ms)	A_i (–)	$\langle\mathcal{M}\rangle$ (m/s)	$\langle\mathcal{M}\rangle\, R_c/D$ (–)	$\xi_{i\,N}$ (nm)	$\xi_{i\,R}$ (nm)	D_g (m^2/s)	α (–)
AGAR								
$A_{1\%}$	135	100	3.5×10^{-7}	1.34×10^{-6}	24.8	13.3	2.07×10^{-9}	1.11
$A_{1.5\%}$	93	100	3.4×10^{-7}	0.98×10^{-6}	20.2	8.5	2.02×10^{-9}	1.13
$A_{2\%}$	65	100	3.6×10^{-7}	0.91×10^{-6}	17.4	7.1	2.07×10^{-9}	1.11
AGAR in contact with initially dry pectin films for 1–6 h								
$A_{2\%}P_{1h}$	51	100	3.7×10^{-7}	0.81×10^{-6}	15.4	7.0	1.90×10^{-9}	1.21
$A_{2\%}P_{2h}$	49	100	3.8×10^{-7}	0.84×10^{-6}	15.4	7.0	1.85×10^{-9}	1.24
$A_{2\%}P_{3h}$	53	100	3.5×10^{-7}	0.77×10^{-6}	15.4	7.4	1.86×10^{-9}	1.24
$A_{2\%}P_{4h}$	49	100	3.8×10^{-7}	0.83×10^{-6}	15.3	6.8	1.75×10^{-9}	1.31
$A_{2\%}P_{5h}$	54	100	3.4×10^{-7}	0.76×10^{-6}	15.3	6.8	1.82×10^{-9}	1.27
$A_{2\%}P_{6h}$	47	100	3.9×10^{-7}	0.86×10^{-6}	15.3	7.1	1.86×10^{-9}	1.24
AGAR in contact with initially dry pectin–alginate films for 1–6 h								
$A_{2\%}PAL_{1h}$	30	100	6.0×10^{-7}	1.31×10^{-6}	15.2	8.0	1.78×10^{-9}	1.29
$A_{2\%}PAL_{2h}$	35	100	5.1×10^{-7}	1.31×10^{-6}	15.2	8.1	1.84×10^{-9}	1.25
$A_{2\%}PAL_{3h}$	41	100	4.3×10^{-7}	0.99×10^{-6}	15.0	8.1	1.86×10^{-9}	1.24
$A_{2\%}PAL_{4h}$	27	100	6.6×10^{-7}	1.40×10^{-6}	15.0	7.3	1.74×10^{-9}	1.32
$A_{2\%}PAL_{5h}$	35	100	4.8×10^{-7}	1.00×10^{-6}	15.0	7.8	1.84×10^{-9}	1.25
$A_{2\%}PAL_{6h}$	36	100	4.9×10^{-7}	1.10×10^{-6}	14.9	7.5	1.82×10^{-9}	1.26

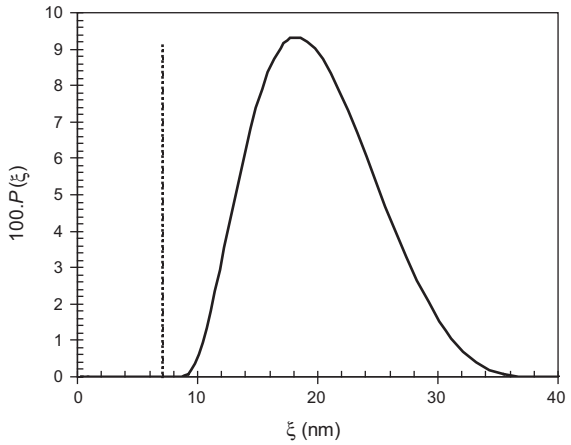

Fig. 7. LF-NMR evaluation of the continuous mesh size distribution [solid line, Eq. (15)] referring to the 2.00% w/w native agar gel. $P(\xi)$ is the occurrence probability of a mesh whose diameter is ξ. The dotted line indicates the ξ evaluation according to the rheological approach [Eq. (4)].

after about 1 h (see Fig. 5A). The small amount of absorbed water is the reason for the very low $\bar{\xi}$ values (from both the rheology, $\xi_{i\ R}$, and the LF NMR, $\xi_{i\ N}$, point of view, see Table 5) and the reduction of D_g with respect to the values competing to the agar gel. In turn, this reflects in an increase of network tortuosity that, in this case, grows up to about 1.5. The D_g independence on the diffusion time t_d indicates the existence of interconnected meshes.

When initially dry PAL film is considered, the water loss experienced by the agar gel, whatever the time considered, is about 2.5 times that competing to the case of the P film (see Fig. 5A). This effect translates into a reduction of the water protons relaxation time (T_{2i}) with respect to the case of $A_{2\%}P$ (see Table 4). As the decrease of the average mesh size ($\bar{\xi} = \xi_{i\ N}$) according to Eq. (9) is not equally evident (see Table 4), it turns out an increase of the relaxivity $\langle\mathcal{M}\rangle$. This indicates a small dependence of $\langle\mathcal{M}\rangle$ on the gel swelling degree that could be explained by the different accessibility of particular chemical groups (present on the agar chains) by water molecules in dependence of the swelling degree. Also in this case, from the mesh size point of view, the agar network is homogeneous, meshes are interconnected (D_g is t_d independent) and network tortuosity is comparable to that of the agar gel facing to pectin. Finally, the LF-NMR estimation of the average mesh size is about two times that coming from the rheological approach (see Table 4) and the low values of the dimensionless parameter $\langle\mathcal{M}\rangle\ R_c/D_g$ ensure the attainment of the fast diffusion conditions. Interestingly, water absorption by the PAL film comports a considerable variation of the relaxation behavior of the water protons trapped inside the PAL network. Indeed, in dry conditions, PAL film is characterized by only one relaxation time (2 ms) while relaxation times grow up to two/three after, at least, one hour contact with the agar gel. In addition, the mean relaxation time greatly increases with respect to the dry condition (almost two orders of magnitude, see Table 5). This means that the presence of alginate (and the lower glycerol content) considerably improves the hydrophilic character of the sample, this being proved by Fig. 5A showing the amount of water gained by the PAL film at different contact times. The presence of two/three relaxation times evidences the existence of mesh classes differing for the average mean size ($\xi_{i\ N}$) and relative abundance (A_i) (see Table 5). Thus, the PAL network is structurally much more complex than that pertaining to the agar and P systems and this seems reasonable in the light of the presence of two different polymeric chains that give origin to an interpenetrated network. It seems interesting to underline the fact that the rheological estimation of the average mesh size ($\xi_{i\ R}$) is almost coincident with the LF-NMR estimation of the mesh size corresponding to the most abundant class (≈80%, $\xi_{2\ N}$), whatever the contact time. The almost constant values assumed by both $\xi_{i\ R}$ and $\xi_{2\ N}$ over the 6 h reflects the fact that after 1 h, PAL swelling is almost complete and no further variation of mesh size occurs. The higher amount of water absorbed by the PAL film reflects in a higher D_g (and, thus, in a lower tortuosity) with respect to the P film case. Also in this case,

Table 5
Low field NMR parameters referring to the Pectin (P) and pectin–alginate (PAL) films after contact with the 2.00% agar gel for different times (1–6 h). T_{2i} and A_i are, respectively, the ith water protons relaxation time and its relative abundance, $\langle\mathcal{M}\rangle$ is relaxivity, $\langle\mathcal{M}\rangle\ R_c/D$ is a dimensionless parameter indicating fast diffusion conditions when it is $\ll 1$, $\xi_{i\ N}$ and $\xi_{i\ R}$ are, respectively, the average mesh size according to the low filed NMR and the rheological approach, D_g is the water self diffusion coefficient inside the gel and α is the polymeric network tortuosity.

	T_{2i} (ms)	A_i (–)	$\langle\mathcal{M}\rangle$ (m/s)	$\langle\mathcal{M}\rangle\ R_c/D$ (–)	$\xi_{i\ N}$ (nm)	$\xi_{i\ R}$ (nm)	D_g (m^2/s)	α (–)
PECTIN film in contact with AGAR for 1–6 h								
P_{1h}	13	100	0.60×10^{-7}	0.04×10^{-6}	3.4	2.5	1.54×10^{-9}	1.49
P_{2h}	14	100	0.66×10^{-7}	0.04×10^{-6}	3.8	2.4	1.57×10^{-9}	1.46
P_{3h}	13	100	0.77×10^{-7}	0.05×10^{-6}	3.9	2.2	1.51×10^{-9}	1.53
P_{4h}	15	100	0.75×10^{-7}	0.05×10^{-6}	4.2	2.9	1.54×10^{-9}	1.49
P_{5h}	14	100	0.89×10^{-7}	0.06×10^{-6}	4.4	2.3	1.65×10^{-9}	1.39
P_{6h}	14	100	0.98×10^{-7}	0.07×10^{-6}	3.5	2.6	1.53×10^{-9}	1.50
Pectin–alginate film in contact with AGAR for 1–6 h								
PAL_{1h}	344	7	0.56×10^{-7}	0.08×10^{-6}	40.4	8.0	1.83×10^{-9}	1.25
	80	79			8.5			
	46	14			4.8			
PAL_{2h}	198	13	0.66×10^{-7}	0.10×10^{-6}	24.3	6.9	1.85×10^{-9}	1.24
	68	87			7.9			
PAL_{3h}	315	12	0.53×10^{-7}	0.08×10^{-6}	31.9	7.2	1.92×10^{-9}	1.19
	84	73			7.9			
	45	15			4.1			
PAL_{4h}	290	8	0.61×10^{-7}	0.10×10^{-6}	33.3	6.0	1.84×10^{-9}	1.25
	78	80			8.3			
	46	12			4.9			
PAL_{5h}	358	12	0.49×10^{-7}	0.08×10^{-6}	33.6	7.2	1.91×10^{-9}	1.21
	93	72			8.0			
	55	16			4.5			
PAL_{6h}	394	9	0.68×10^{-7}	0.10×10^{-6}	52.5	6.1	1.93×10^{-9}	1.19
	81	71			9.6			
	46	20			5.4			

the D_g independence on the diffusion time indicates that meshes are interconnected.

4. Conclusions

The diffusivity of the AA from antioxidant active interfaces like P or PAL edible films to foods can be studied by using agar gels that mimic a viscoelastic solid-hydrophilic phase. Primarily, the understanding of the nano- and microstructure of the polymeric matrices involved in the mass transport phenomenon is a very important feature for the description of networks and, therefore, very useful for the understanding of the delivery properties of film matrices.

Starting from dynamic tests performed under linear and non linear conditions, the 2.00% w/w-agar concentration was selected to develop the viscoelastic solid food model to be assayed, because it ensures strong gel properties.

Rheological studies carried out on the 2.00% w/w-agar gel and the edible film indicated that calcium-junction zones of P and PAL film matrices are stronger than the physical interactions in the agar hydrated network, especially after dehydration for film casting. Besides, P network is characterized by a higher number of calcium-junction zones than in PAL matrix, in spite of the higher glycerol (plasticizer) content of P film. The proportion of water absorbed by the P-film is noticeably lower (12%) than the water absorbed by PAL-film (42%), and a higher number of physical interactions characterizes the less hydrated pectin chains of P film. Consequently, P film seems to be more useful as an interface applied on intermediate moisture foods since its microstructure is better preserved during contact due to the lower water absorption capacity. In spite of its higher glycerol content, the elasticity was similar to that observed for PAL films before contact (0 h) with the 2.00% w/w agar gel. The LF-NMR characterization reveals the existence of homogeneous, nano-sized and interconnected network in the case of agar and P film, while a more complex structure was seen for PAL films.

The mesh size $\bar{\xi}$ of the P and PAL films increased in the first hour contact with agar 2.00% gel and, then, it remained, substantially, constant. However, the higher degree of swelling (42%) suffered by the PAL film led to a higher $\bar{\xi}$, either determined by rheology or LF-NMR relaxometry, as well as to a considerable higher water mobility in the film network. The LF-NMR evaluation of $\bar{\xi}$ resulted to be about 1.5–2 times that coming from the rheological approach. However, this does not seem a big difference as the rheological evaluation represents the lower value of the continuous mesh size distribution evaluated by LF-NMR.

Both mesh size and water mobility that characterize the microstructures of films and of the 2.00%-agar (receptor) gels are main parameters that should be considered affecting the release of AA from the film networks to the agar gels, as well as the diffusion of AA into the agar gel or food.

Acknowledgements

Maria De'Nobili and Ana Rojas are grateful to the University of Buenos Aires, National Research Council of Argentina (CONICET) and Agencia Nacional de Promoción Científica y Tecnológica (ANPCyT). Michela Abrami, Romano Lapasin and Mario Grassi thank the Italian Ministry of Education (PRIN 2010-11 (20109PLMH2)).

References

Abrami, M., D'Agostino, I., Milcovich, G., Fiorentino, S., Farra, R., Asaro, F., Lapasin, R., Grassi, G., Grassi, M., 2014. Physical characterization of alginate–Pluronic F127 gel for endoluminal NABDs delivery. Soft Matter 10, 729–737.

Arnott, S., Fulmer, A., Scott, W.E., 1974. The agarose double helix and its function in agarose gel structure. J. Mol. Biol. 90, 269–284.

Braccini, I., Pérez, S., 2001. Molecular basis of Ca^{2+}-induced gelation in alginates and pectins: the egg box model revisited. Biomacromolecules 2, 1089–1096.

Chui, M.M., Phillips, R.J., McCarthy, M.J., 1995. Measurement of the porous microstructure of hydrogels by nuclear magnetic resonance. J. Colloid Interface Sci. 174, 336–344.

Coviello, T., Matricardi, P., Alhaique, F., Farra, R., Tesei, G., Fiorentino, S., Asaro, F., Milcovich, G., Grassi, M., 2013. Guar gum/borax hydrogel: rheological, low field NMR and release characterizations. Exp. Polym. Lett. 7, 733–746.

De'Nobili, M.D., Perez, C.D., Navarro, D.A., Stortz, C.A., Rojas, A.M., 2011. Hydrolytic stability of L-(+)-ascorbic acid in low methoxyl pectin films with potential antioxidant activity at food interfaces. Food Bioprocess Technol. 6, 186–197.

De'Nobili, M.D., Curto, L.M., Delfino, J.M., Soria, M., Fissore, E.N., Rojas, A.M., 2013. Performance of alginate films for retention of L-(+)-ascorbic acid. Int. J. Pharm. 450, 95–103.

Djabourov, M., Clark, A.H., Rowlands, D.W., Ross-Murphy, S.B., 1989. Small angle X-ray scattering characterization of agarose sols and gels. Macromolecules 22, 180–188.

Draper, N.R., Smith, H., 1966. Applied Regression Analysis. John Wiley & Sons Inc, New York.

Flory, P.J., 1953. Principles of Polymer Chemistry. Cornell University Press, Ithaca, USA.

Grassi, M., Grassi, G., Lapasin, R., Colombo, I., 2007. Understanding Drug Release and Absorption Mechanisms: A Physical and Mathematical Approach. CRC Press, Boca Raton, FL, USA, pp. 1–627.

Grassi, M., Fiorentino, S., Farra, R., Dapas, B., Grassi, G., 2015. Hydrogels mesh size evaluation. In: Matricardi, P., Alhaique, F., Coviello, T. (Eds.), Polysaccharide Hydrogels: Characterization and Biomedical Applications. Pan Stanford Publishing, Singapore, pp. 139–165, Chapter 4.

Han, J.H., 2005. In: Jung H. Han (Ed.), Innovations in Food Packaging. Elsevier Ltd.

Holz, M., Heil, S.R., Sacco, A., 2000. Temperature-dependent self-diffusion coefficient of water and six selected molecular liquids for calibration in accurate H NMR PFG measurements. Phys. Chem. 2, 4740–4742.

Hyun, K., Kim, S.H., Ahn, K.H., Lee, S.J., 2002. Large amplitude oscillatory shear as a way to classify the complex fluids. J. Non-Newtonian Fluid Mech. 107, 51.

Jothisaraswathi, S., Babu, B., Rengasamy, R., 2006. Seasonal studies on alginate and its composition II: Turbinaria conoides (J.Ag.) Kutz. (Fucales, Phaeophyceae). J. Appl. Phycol. 18, 161–166.

Klöck, G., Pfefferrnann, A., Ryser, C., Gröhn, P., Kuttler, B., Hahn, H.J., Zimmermann, U., 1997. Biocompatibility of mannuronic acid-rich alginates. Biomaterials 18, 707–713.

Kouwijzer, M., Pérez, S., 1998. Molecular modeling of agarose helices, leading to the prediction of crystalline allomorphs. Biopolymers 46, 11–29.

Kuijpers, A.J., Engbers, G.H.M., Feijen, J., De Smedt, S.C., Meyvis, T.K.L., Demeester, J., Krijgsveld, J., Zaat, S.A.J., Dankert, J., 1999. Characterization of the network structure of carbodiimide cross-linked gelatin gels. Macromolecules 32, 3325–3334.

Labropoulos, K.C., Niesz, D.E., Danforth, S.C., Kevrekidis, P.G., 2002. Dynamic rheology of agar gels: theory and experiments part I development of a rheological model. Carbohydr. Polym. 50, 393–406.

Lapasin, R., Pricl, S., 1995. Rheology of Industrial Polysaccharides. Theory and Applications. Blackie Academic and Professional, Chapman and Hall, Wester Cleddens Road, Bishopbriggs, Glasgow G64 2NZ, UK, pp. 85–103.

Lapasin, R., Grassi, M., Coceani, N., 2001. Effects of polymer addition on the rheology of o/w emulsions. Rheol. Acta 40, 185–192.

Latour, L., Mitra, P.P., Kleinberg, R.L., Sotak, C.H., 1993. Time dependent diffusion coefficient of fluids in porous media as a probe of surface-to-volume ratio. J. Magnetic Resonance 101, 342–346.

Lee, K.Y., Mooney, D.J., 2012. Alginate: properties and biomedical applications. Prog. Polym. Sci. 37, 106–126.

Pasut, E., Toffanin, R., Voinovich, D., Pedersini, C., Murano, E., Grassi, M., 2008. Mechanical and diffusive properties of homogeneous alginate gels in form of particles and cylinders. J. Biomed. Mater 87, 819–824.

Pérez, S., Mazeau, K., Hervé du Penhoat, C., 2000. The three-dimensional structures of the pectic polysaccharides. Plant Physiol. Biochem. 38 (1/2), 37–55.

Pérez, C.D., De'Nobili, M.D., Rizzo, S.A., Gerschenson, L.N., Descalzo, A.M., Rojas, A.M., 2013. High methoxyl pectin–methyl cellulose films with antioxidant activity at a functional food interface. J. Food Eng. 116, 162–169.

Provencher, S.W.A., 1982. Constrained regularization method for inverting data represented by linear algebraic or intergral equations. Comput. Phys. Comm. 27, 213.

Scherer, G.W., 1994. Hydraulic radius and mesh size of gels. J. Sol–Gel. Sci. Technol. 1, 285–291.

Schurz, J., 1991. Rheology of polymer solutions of the network type. Prog. Polym. Sci. 16 (1), 1–53.

Sim, H.G., Ahn, K.H., Lee, S.J., 2003. Large amplitude oscillatory shear behavior of complex fluids investigated by a network model: a guideline for classification. J. Non-Newtonian Fluid Mech. 112, 237–250.

Sokal, R.R., Rohlf, J.B., 2000. Biometry. The Principles and Practice of Statistics in Biological Research. WH Freeman and Company, San Francisco, pp. 253–380.

Soskey, P.R., Winter, H.H., 1984. Large step shear strain experiments with parallel-disk rotational rheometers. J. Rheol. 28, 625–645.

Stabler, C., Wilks, K., Sambanis, A., Constantinidis, I., 2001. The effects of alginate composition on encapsulated _TC3 cells. Biomaterials 22, 1301–1310.

Turco, G., Donati, I., Grassi, M., Marchiali, G., Lapasin, R., Paoletti, S., 2011. Mechanical spectroscopy and relaxometry on alginate hydrogels. A comparative analysis for structural characterization and network mesh size determination. Biomacromolecules 12, 1272–1282.

Vincken, J.P., Schols, H.A., Oomen, R.J.F.J., McCann, M.C., Ulvskov, P., Voragen, A.G.J., Visser, R.G.F., 2003. If homogalacturonan were a side chain of rhamnogalacturonan I. Implications for cell wall architecture. Plant Physiol. 132 (4), 1781–1789.

Voragen, A.G.J., Coenen, G.J., Verhoef, R.P., Schols, H.A., 2009. Pectin, a versatile polysaccharide present in plant cell walls. Struct. Chem. 20, 263–275.

Wang, X., Ni, Q., 2003. Determination of cortical bone porosity and pore size distribution using a low field pulsed NMR approach. J. Orthopaedic Res. 21, 312–319.

Whittal, K.P., MacKay, A.L., 1989. Quantitative interpretation of NMR relaxation data. J. Magnetic Resonance 84, 134–152.

Willats, W.G.T., Knox, J.P., Mikkelsen, D., 2006. Pectin: new insights into an old polymer are starting to gel. Trends Food Sci. Technol. 17, 97–104.